

Spin-charge separation in the quantum boomerang effect

Pablo Capuzzi,^{1,2} Luca Tessieri,³ Zehra Akdeniz,⁴ Anna Minguzzi,⁵ and Patrizia Vignolo^{6,7}

¹*Departamento de Física, Facultad de Ciencias Exactas y Naturales, Universidad de Buenos Aires, Pabellón 1, Ciudad Universitaria, 1428 Buenos Aires, Argentina*

²*Instituto de Física de Buenos Aires (UBA-CONICET),*

Pabellón 1, Ciudad Universitaria, 1428 Buenos Aires, Argentina

³*Instituto de Física y Matemáticas, Universidad Michoacana de San Nicolás de Hidalgo, 58060, Morelia, Mexico*

⁴*Faculty of Science and Letters, Piri Reis University, 34940 Tuzla, Istanbul, Turkey*

⁵*Univ. Grenoble Alpes, CNRS, LPMMC, 38000 Grenoble, France*

⁶*Université Côte d'Azur, CNRS, Institut de Physique de Nice, 06200 Nice, France*

⁷*Institut Universitaire de France*

We study the localization dynamics of a SU(2) fermionic wavepacket launched in a (pseudo)random potential. We show that in the limit of strong inter-component repulsions, the total wavepacket exhibits a boomerang-like dynamics, returning near its initial position as expected for non-interacting particles, while separately each spin-component does not. This spin-charge separation effect occurs both in the infinite repulsive limit and at finite interactions. At infinite interactions, the system is integrable and thermalization cannot occur: the two spin-components push each other during the dynamics and their centers of mass stop further from each other than their initial position. At finite interactions, integrability is broken, the two spin-components oscillate and mix, with their center-of-mass positions converging very slowly to the center of mass of the whole system. This is a signature that the final localized state is a fully spin-mixed thermalized state.

I. INTRODUCTION

In disordered quantum systems it has been shown that a wavepacket launched with some initial velocity may return to its initial position and stop there. This phenomenon, known as the quantum boomerang effect (QBE) [1–3], occurs in the Anderson localization (AL) limit when interactions are completely negligible and disorder completely freezes the dynamics of the wavepacket [4, 5]. The QBE is found not only in real space, but also in momentum space. In this latter case, the (pseudo)-disorder in momentum space is introduced by kicking periodically the wavepacket. Indeed, the first experimental evidence of the QBE was obtained in a quantum kicked-rotor experiment [3]. These measurements have confirmed the theoretical predictions [1, 2] and elucidated the crucial role of the time-reversal symmetry in determining the presence or absence of the QBE. In fact, the occurrence of the QBE requires not only the system to be in the AL regime, but also that some symmetries of the Hamiltonian and of the initial state of the wavepacket are fulfilled [6–8]. When localization takes place in momentum space, as in the case of the kicked rotor, it is the time-reversal symmetry that is crucial for the wavepacket to come back to its initial position. On the other hand, for systems that localize in real space, like the Anderson model, it is the space-time reversal symmetry that regulates the dynamics of the quantum boomerang [6, 8]. When this symmetry is broken, the wavepacket –after having been launched– stops somewhere but not necessarily in its initial position.

Like Anderson localization, QBE is a phenomenon that is expected for non-interacting systems, both bosonic and fermionic. It has been shown that weak interactions between particles partially destroy QBE: the center of mass of the wavepacket makes a U-turn, but without coming back to its initial position [9]. This also happens for a one-dimensional (1D) strongly interacting Bose gas, which can be mapped to a weakly interacting Fermi gas [10]: interactions partially de-

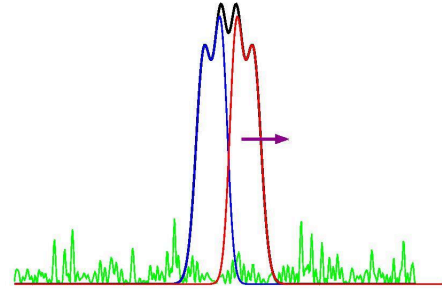


FIG. 1: Schematic representation of the system studied in this work: a spatially spin-demixed initial state is realized with an initial non-vanishing momentum in a disorder potential.

stroy interference effects and thus the QBE. However, in the limit where the interactions are infinitely repulsive, namely in the Tonks-Girardeau regime, the QBE holds since the system can be mapped onto free fermions [10].

In this paper, we investigate the quantum boomerang dynamics of a strongly repulsive two-component Fermi gas (see Fig. 1). The underlying idea is to explore a system where different spin configurations are available and study if the QBE, or its failure, can bring information about the thermalization of the system and, possibly, whether its final state is many-body localized [11–13].

A two-component Fermi gas with strong, repulsive inter-component contact interactions can be mapped onto an effective spin-chain Hamiltonian where the spins exchange when particles of different spin-components collide [14]. The dynamics of such a system starting from an initially spin-demixed configuration have been studied in the absence of disorder [15–17], highlighting the short-time superdiffusive dynamics of the magnetization interface for two spin-components happens in a similar way in spin chains [18–21].

It has also been shown that such a system relaxes towards the microcanonical ensemble during a time interval that increases with the number of particles, integrability being broken by the presence of an external potential at finite interactions [17].

The presence of the disorder localizes the whole wavepacket as well as the two spin components. The size of the wavepacket for each spin-component is initially half of the total size, but very rapidly the two spin-components mix so that their size quickly reaches that of the total wavepacket. Simultaneously, the center of mass of the whole system does a U-turn and stops at its initial position, as if the system were non-interacting. Instead, the center-of-mass of each spin-component does not return to its initial position but, in the presence of finite interactions, converges towards the position of the center-of-mass of the whole system, with a damped oscillating dynamics much slower than that of the whole density. This separation of time scales is due to the fact that the spin dynamics is governed by the inverse of the interaction strength, which is very large in our model. We therefore observe a charge-spin separation in the QBE.

Moreover, at finite interactions, where spin mixing occurs, we find that the final localized spin densities are those expected in the microcanonical ensemble. Whereas, in the limit of infinite interaction strength, where the center of mass of two spin-component stop further apart from their initial positions, the final localized state is very different from that expected in the microcanonical ensemble because integrability prevents thermalization.

The manuscript is organized as follows. The physical model is introduced in Sec. II, where we remind how the system can be mapped onto a spin-chain model and the dynamics can be exactly solved in the strong-interacting limit. Then, the boomerang experiment is described in Sec. III, where we detail a proposal for an experimental protocol and analyze the results, discussing the role of the interactions and of the symmetries. The thermalization issue is discussed in Sec. IV. Concluding remarks are given in Sec. V.

II. THE MODEL

We consider a $SU(2)$ fermionic mixture with $N_\uparrow(N_\downarrow) = N/2$ fermions in the spin-up (spin-down) component. Each fermion is subject to an external potential $V(x)$ and interacts with fermions of the other spin component via a repulsive contact potential of strength g . Thus, the many-body Hamiltonian reads

$$\mathcal{H} = \mathcal{H}_0 + \sum_{i=1}^{N_\uparrow} \sum_{j=N_\uparrow+1}^N g \delta(x_i - x_j) \quad (1)$$

with

$$\mathcal{H}_0 = \sum_{i=1}^N \left[-\frac{\hbar^2}{2m} \frac{\partial^2}{\partial x_i^2} + V(x_i) \right]. \quad (2)$$

Close to the fermionized regime, where interactions are so large that they play the role of a Pauli principle between

fermions belonging to different spin components, the many-body wavefunction can be written as [22]

$$\Psi(X) = \sum_{P \in S_N} a_P \theta_P(X) \Psi_A(X) \quad (3)$$

where the summation is performed over all P permutations of N elements, S_N . The vector $X = (x_{1,\sigma_1}, \dots, x_{N,\sigma_N})$ includes particle coordinates x_i and spin indices σ_i , $\Psi_A(X;t)$ is the zero-temperature solution for spinless fermions obeying the non-interacting Hamiltonian \mathcal{H}_0 , and $\theta_P(X)$ is the generalized Heaviside function, which is equal to 1 in the coordinate sector $x_{P(1),\sigma_{P(1)}} < \dots < x_{P(N),\sigma_{P(N)}}$ and zero otherwise. The coefficients a_P are determined by minimizing the energy [22]:

$$E = E_\infty + \frac{1}{g} \left(\frac{\partial E}{\partial g^{-1}} \right)_{1/g \rightarrow 0} = E_\infty - \frac{\mathcal{C}}{g}, \quad (4)$$

with $\mathcal{C} = -(\partial E / \partial g^{-1})_{1/g \rightarrow 0}$ being the Tan's contact up to a dimensional constant. This is equivalent to solving the eigenvalue problem of the effective Hamiltonian

$$\mathcal{H}_{\text{eff}} = \mathcal{H}|_{1/g \ll 1} = E_\infty \hat{1} + H_S \quad (5)$$

obtained by expanding \mathcal{H} on the $\{\phi_n\}$ snippet basis, namely the basis of all particle sectors obtained by global permutations modulo the permutations of identical fermions with the same spin [23]. Furthermore, it has been shown that H_S is equivalent to a spin chain Hamiltonian in position particle space [14]

$$H_S = \sum_{j=1}^{N-1} (-J_j \hat{1} + J_j \hat{P}_{j,j+1}) \quad (6)$$

where $\hat{P}_{j,j'} = (\vec{\sigma}^{(j)} \vec{\sigma}^{(j')} + 1)/2$ is the permutation operator and $\vec{\sigma}^{(j)} = (\sigma_x^{(j)}, \sigma_y^{(j)}, \sigma_z^{(j)})$ are the Pauli matrices. The hopping terms J_i in Eq. (6) can be written as

$$J_i = \frac{N!}{g} \int_{-\infty}^{\infty} dX \delta(x_i - x_{i+1}) \theta_{\text{id}}(X) \left| \frac{\partial \Psi_A}{\partial x_i} \right|^2. \quad (7)$$

A. The dynamics close to the fermionized regime

In an out-of-equilibrium situation, when the free-fermion part of the wavefunction Ψ_A is time-dependent, the J_j terms (7) change in time. Therefore, to obtain $\Psi(X, \bar{t} + dt)$ starting from $\Psi(X, \bar{t})$ we proceed as follows [24]. We start by finding $J_i(\bar{t})$ to determine the spin-chain Hamiltonian at a time \bar{t} . By diagonalizing $H_S(\bar{t})$ we obtain the eigenvectors $a_P^{(j)}(\bar{t})$ and their corresponding eigenvalues $\mathcal{E}_j(\bar{t})$. Expanding the coefficients a_P of Eq. (3) in this basis gives the identity $a_P(\bar{t}) = \sum_j \alpha_j(\bar{t}) a_P^{(j)}(\bar{t})$ and makes it possible to compute the coefficients at a time $\bar{t} + dt$ as

$$a_P(\bar{t} + dt) = \sum_j \alpha_j(\bar{t}) e^{-i\mathcal{E}_j(\bar{t})dt/\hbar} a_P^{(j)}(\bar{t}). \quad (8)$$

Once the evolved coefficients (8) are known, the many-body wavefunction at a time $\bar{t} + dt$ can be written as

$$\Psi(X; \bar{t} + dt) = \sum_{P \in S_N} a_P(\bar{t} + dt) \theta_P(X) \Psi_A(X; \bar{t} + dt). \quad (9)$$

For this approach to work, the time steps need to fulfil the condition $dt \ll \hbar/|J_j(\bar{t} + dt) - J_j(\bar{t})|$ for any \bar{t} and any j . Once the many-body wavefunction is calculated, we can compute the spin densities at each time

$$\rho_{\uparrow, \downarrow}(x, t) = \sum_i \delta_{\sigma_i}^{\uparrow, \downarrow} \sum_{P \in S_n} |[a_P(t)]_i|^2 \rho^i(x, t) \quad (10)$$

where

$$\rho^i(x, t) = \int_{x_1 < \dots < x_{i-1} < x < x_{i+1} \dots < x_N} dX \delta(x - x_i) |\Psi_A(X, t)|^2$$

is the density in the sector $x_1 < \dots < x_{i-1} < x < x_{i+1} \dots < x_N$, while the total density is $\rho(x, t) = \sum_{i=1}^N \rho_i(x, t) = \rho_{\uparrow}(x, t) + \rho_{\downarrow}(x, t)$.

B. The dynamics in the presence of disorder

We now focus our attention to the case of a wavepacket of fermions initially prepared at equilibrium in a harmonic trap of frequency ω , which is then released with an imprinted initial momentum $\hbar k_0$ on each fermion and propagates in the pseudorandom potential

$$V_{\text{dis}}(x) = \mathcal{W} \sin(\sqrt{5}\pi(x + i_c L/2))^3 / (a_{\text{ho}}/10)^3 \quad (11)$$

where \mathcal{W} is the potential amplitude, $a_{\text{ho}} = \sqrt{\hbar/(m\omega)}$ the typical harmonic potential length scale, L the size of the system, and i_c an integer index that counts the pseudo-disorder configurations. It has already been shown that the potential (11), defined on a lattice, induces both Anderson localisation [25] and the boomerang effect [2] as a truly random potential. We choose the potential (11), rather than a truly random one, because of its relevance to cold-atom experiments, in which pseudo-random potentials can be realized with appropriate laser configurations [26]. We would like to stress, however, that we have verified that the results described in this paper are still valid if the pseudo-random potential (11) is replaced with a random potential of adequate strength [2]. The potential (11) has zero average $\overline{V_{\text{dis}}(x)} = 0$ and is delta-correlated $\overline{V_{\text{dis}}(x)V_{\text{dis}}(x')} = \gamma\delta(x - x')$. The values obtained from Eq. (11) by keeping x fixed and varying i_c have a uniform probability distribution function (PDF). Here and in the rest of this paper, we use the symbol $\overline{(\dots)}$ to denote the average over a sequence of pseudo-disorder configurations (we consider different i_c values in Eq. (11)).

The disorder strength γ determines the mean-free path ℓ and the mean-free time τ for a non-interacting system. Indeed, we remind that for a wavepacket with a momentum $\hbar k_0$ in the Born approximation, one has [1]

$$\ell = \frac{\hbar^4 k_0^2}{2m^2 \gamma}, \quad \text{and} \quad \tau = \frac{\hbar^3 k_0}{2m\gamma}. \quad (12)$$

Here and in the following, we have fixed $\gamma = 0.86 \cdot 10^3 \hbar^2 \omega^2 a_{\text{ho}}$, and $k_0 = 50/a_{\text{ho}}$, that imply $\ell = 1.45 a_{\text{ho}}$ and $\tau = 0.029 \omega^{-1}$. We remark that, in order to use such expressions for the case of N non-interacting fermions, $(\hbar k_0)^2 / (2m)$ has to be much larger than the energy of the highest occupied orbital [10], namely the Fermi energy of the system.

The presence of disorder significantly influences the time evolution of the hopping terms J_i . In an experiment in which the wavepacket is first prepared separately in a deterministic initial condition and then left to evolve in a disordered potential, the J_i 's at time $t = 0$ are determined by the initial state and their PDFs are Dirac deltas (as shown in the first panel of Fig. 2). Because the fermions move in a (pseudo)-random potential, the hopping terms become stochastic variables, with disorder entering via the time evolution of Ψ_A . As a consequence, at each time t , the statistical properties of the J_i terms must be described with a PDF $P(J_i)$. The time evolution of the corresponding marginal PDFs is depicted in Fig. 2, which shows that initially the PDFs broaden and drift towards higher values of J_i , eventually reaching a stable asymptotic forms at longer times. These qualitative features are evinced by the time evolution of the average values of the J_i 's and of their rescaled standard deviations

$$\frac{\sigma_{J_i}}{\bar{J}_i} = \frac{\sqrt{\bar{J}_i^2 - \bar{J}_i^2}}{\bar{J}_i}. \quad (13)$$

as shown in Fig. 3.

We can estimate the dependence of the mean-free path ℓ_j and of the mean-free time τ_j on \bar{J}_i and σ_{J_i} for the spin dynamics by using the expression for the localization length for a lattice system with random off-diagonal disorder, derived in the Born approximation [2]. This would give

$$\ell_j \propto \frac{\bar{J}_i^2}{\sigma_{J_i}^2}, \quad \text{and} \quad \tau_j \propto \frac{\bar{J}_i}{\sigma_{J_i}}. \quad (14)$$

Equations (14) predict that ℓ_j does not depend on the strength of the interactions g , whereas τ_j increases with it ($\tau_j \propto g$), which is in agreement with the results presented in the next section.

Finally, let's discuss the stochastic properties of the $J_i(t)$'s. They are ultimately shaped by the random potential $V_{\text{dis}}(x)$, but, unfortunately, the determinantal form of Ψ_A makes highly non-trivial to establish a link between the randomness of the potential $V_{\text{dis}}(x)$ and the stochastic features of the J_i terms. As shown by Eq. (7), the magnitude of the J_i 's is proportional to the sharpness of the cusps, namely, the slope of the wavefunction $\Psi_A(X)$ when two particles approach each other. Therefore, we expect that their average values should strongly depend on the specific features of the experimental protocol.

In the present case, we consider a wavepacket launched with an initial momentum in a disordered landscape. Our numerical analysis has shown that the marginal PDFs of the J_i terms tend to asymptotic forms characterized by a skewed shape and fat tails.

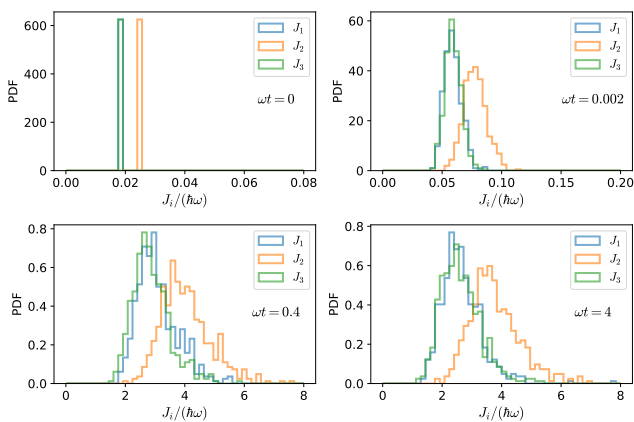


FIG. 2: Evolution of PDF of the J_i terms for the case of an initial deterministic wavepacket of 2+2 fermions, initially prepared in a harmonic trap of frequency ω , launched with an initial momentum $\hbar k_0$ in the presence of a pseudorandom potential (11). The different panels correspond to times: 0, 0.002, 0.4, 4 in units of $1/\omega$.

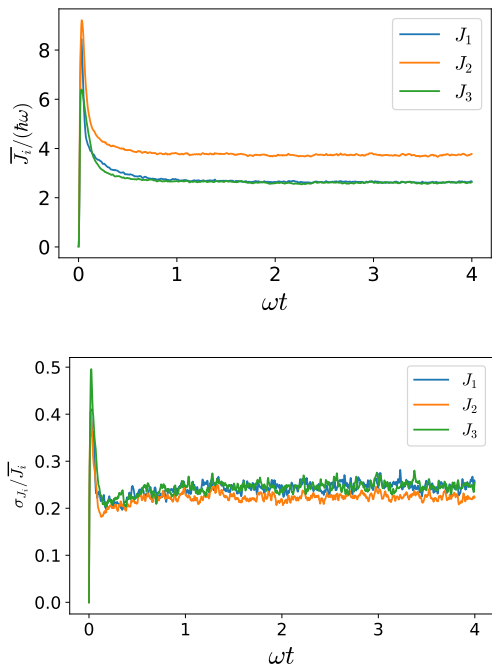


FIG. 3: Average hopping terms \bar{J}_i , for the case $g = 100\hbar\omega a_{\text{ho}}$, (top panel) and relative standard deviation (13) of the hopping terms J_i (bottom panel), as functions of time, for the same experimental protocol as for Fig. 2 and described in Sec. III.

III. THE BOOMERANG DYNAMICS

We propose in this section an experimental protocol to observe QBE. We consider an initially spatial phase-separated SU(2) fermionic mixture with $N_\uparrow = N_\downarrow$ where the up spins are on the left (L), and down spins on the right (R), both trapped in a harmonic potential $V_{\text{ho}} = m\omega^2 x_i^2/2$. At $t = 0$ we release

the fermions in a disorder potential $V_{\text{dis}}(x_i)$ by kicking them towards the right with an initial momentum $\hbar k_0$ and switching off the harmonic potential.

We study the dynamics of the center-of-mass \bar{x} and the width w of the total disordered-averaged density profile

$$\bar{x} = \int \bar{\rho}(x) x dx / N, \quad (15)$$

$$w = \left(\int \bar{\rho}(x) (x - \bar{x})^2 dx / N \right)^{1/2}, \quad (16)$$

and we do the same for each spin component

$$\bar{x}_{\uparrow,\downarrow} = \int \bar{\rho}_{\uparrow,\downarrow}(x) x dx / N_{\uparrow,\downarrow}, \quad (17)$$

$$w_{\uparrow,\downarrow} = \left(\int \bar{\rho}_{\uparrow,\downarrow}(x) (x - \bar{x}_{\uparrow,\downarrow})^2 dx / N_{\uparrow,\downarrow} \right)^{1/2}. \quad (18)$$

Remark that, to simulate such an experimental protocol in the procedure detailed in Sec. II, the time discretization needs to verify $dt < \tau$.

A. Spin-charge separation in the boomerang dynamics

We observe (see Fig. 4) that, in the fermionized regime ($g \rightarrow \infty$), the two components never mix, and they localize independently, repelling each other. Indeed, in this case the hopping terms J_i vanish and

$$\rho_\uparrow^\infty(x, t) = \rho^L(x, t) = \sum_{i=1}^{N_\uparrow} \rho^i(x, t) \quad (19)$$

and

$$\rho_\downarrow^\infty(x, t) = \rho^R(x, t) = \sum_{i=N_\uparrow+1}^N \rho^i(x, t). \quad (20)$$

Moreover, the width of each component is half of the width of the total density, and we observe that the final position of the center-of-mass of each spin-component is $\bar{x}_{\uparrow,\downarrow}^\infty(t \rightarrow \infty) = \pm w/2$.

The dynamical behavior is considerably different when interactions are large but finite: in this case the two spin components undergo mixing during the dynamics, as happens in the absence of the disorder [17] (see Fig. 4). Each spin component is localized by the disordered hoppings, reaching a final width that is the same of the two components (top panel in Fig. 4). Initially, each component moves away over a distance ℓ_{max} , and then it comes back towards the initial position of the center-of-mass of the whole system, performing damped oscillations, around this position. These oscillations are governed by the frequency spectrum of the spin-chain Hamiltonian (6), which yields the lowest non-zero frequency $\omega^* = (J_1 + J_2 - \sqrt{J_1^2 + J_2^2})/\hbar$, where we have used that

long times $J_1 = J_3$. Remark that the turning point ℓ_{max} is the same for the cases $g/(\hbar\omega a_{ho}) = 100$ and 200 , and that the time evolution scales with g , namely $\bar{x}_{\uparrow,\downarrow}(2t)_{2g} = \bar{x}_{\uparrow,\downarrow}(t)_g$, as predicted by Eqs. (14). The localization dynamics occurs on a much longer timescale with respect to that of the total density. In particular, we observe that at long times one has

$$\bar{x}_{\uparrow,\downarrow} = \frac{1}{2}(\bar{x}_{\uparrow}^{\infty} + \bar{x}_{\downarrow}^{\infty}) \pm \frac{1}{2}(\bar{x}_{\uparrow}^{\infty} - \bar{x}_{\downarrow}^{\infty})\mathcal{F}(t), \quad (21)$$

with $\mathcal{F}(t)$ being a function that depends on the average of spin weights only, $|a_p(t)_i|^2 \delta_{\sigma_i}^{\uparrow,\downarrow}$. Indeed, the time scales of the density dynamics and of the spin dynamics being very different (the first being determined by the disorder strength γ and the second by the hoppings J_i that are proportional to ρ^3/g [27, 28]), the average over configurations splits into two independent parts as if the two dynamical processes were uncorrelated (see Appendix A).

The center-of-mass of the total density exhibits the boomerang dynamics: the whole wavepacket moves away over a distance $\sim \ell$ and then comes back to its initial position, while at the same time the wavepacket localizes. However, each spin-component individually does not come back to its initial position, but its center-of-mass position at long times coincides with the center-of-mass of the whole system (bottom panel in Fig. 4).

Remark that the behaviour of the total density does not depend on the value of the interaction strength in the regime we are analysing ($1/g \ll 1$), so that the black curves in Fig. 4 concern the three cases analyzed ($g/(\hbar\omega a_{ho}) = 100, 200, \infty$). We thus observe a spin-charge separation with respect to the boomerang dynamics, both for finite and infinite values of the interaction strength. This result is in agreement with the prediction of spin-charge separation in the localization dynamics for a disordered chain of spin-1/2 fermions [12].

B. Role of the interactions and symmetries

A straightforward interpretation of our results is the following one. In the strongly interacting mixture, the whole density is described by the spinless-fermions solution. Thus, the whole density follows the boomerang dynamics as expected for non-interacting fermions or Tonks-Girardeau bosons [10]. The effect of the interactions manifests itself in the inter spin-component dynamics, but in a very different way depending on whether the interactions are infinite or finite. When the interactions are infinite, each spin component is just a system of non-interacting particles that is not free to propagate everywhere because of the presence of the other component. It localizes at the same time as the whole system, but largely far away from the position of the center-of-mass of the whole system and also largely far away from their initial position. The center-of-mass of each component does not do the boomerang dynamics: each component moves away but does not come back because it is pushed by the other component.

Instead, when the interaction is large but finite, the situation is completely different. The landscape of the disorder felt by the spins completely change. Particles with different spin

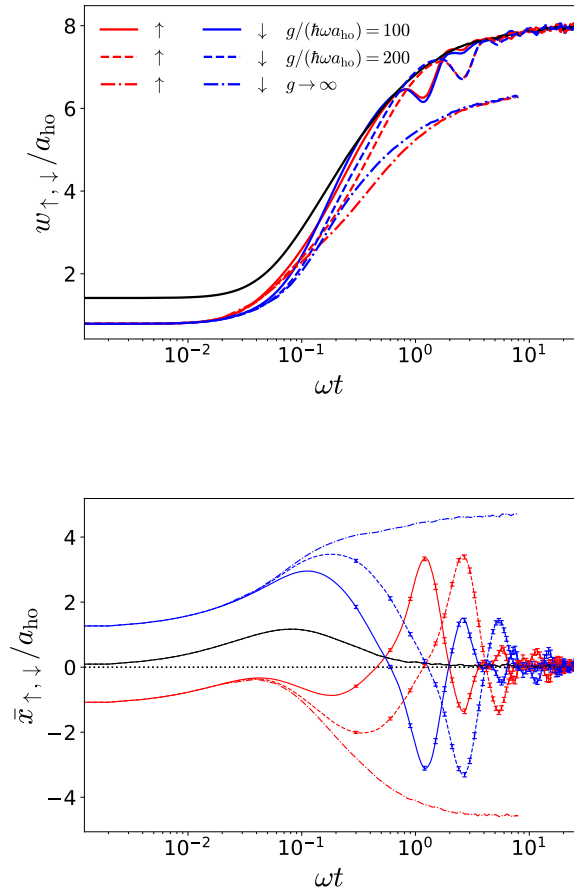


FIG. 4: Disorder-averaged widths w (top panel) and center-of-mass positions (bottom panel) \bar{x} of the whole system (black curve) and of each spin component (red and blue lines) as functions of time (in logscale), for different values of the interaction strengths: $g/(\hbar\omega a_{ho}) = 100$ (continuous lines), $g/(\hbar\omega a_{ho}) = 200$ (dashed lines) and $g \rightarrow \infty$ (dot-dashed lines). Here we used the following parameters: $k_0 a_{ho} = 50$, $\gamma = 0.86 \cdot 10^3 \hbar^2 \omega^2 a_{ho}$, $N = 4$ and we averaged over 512 configurations.

hop with a spatially random probability, that fluctuates as a function of time, and is inversely proportional to the interaction strength. The center-of-mass of each component reaches a final position that is different from the initial one, as already found for other interacting systems [10], and, coincides with that of the whole system.

From the point of view of each component, there is an initial time when the dynamics at finite interactions coincides with that at infinite interactions, but then the trajectories separate, one going back while the other does not. This is very different from what happens with a single-component system [10] where the center-of-mass for the gas of finite interactions slightly deviates from that with infinite interactions.

As a final remark, we would like to highlight the role of symmetries for the QBE. As pointed out in [6, 8], the QBE

takes place in real space if the ensemble of the disordered Hamiltonians $\{\mathcal{H}\}$ is invariant under the action of \mathcal{RT} and if the initial state is an eigenstate of \mathcal{RT} , where \mathcal{R} is the spatial reversal operator and \mathcal{T} the time-reversal operator. For the system we have considered in this work, both conditions are fulfilled. However, each spin component *is not* an eigenstate of \mathcal{RT} . Under the action of \mathcal{RT} the spin-up component on the left is transformed on the spin-down component on the right, and viceversa. Thus, each spin-component separately does not fulfil the condition for the QBE, but the two spin-components system does.

IV. THE THERMALIZATION ISSUE

Given that the system we are studying is characterized by interactions and disorder, it is natural to ask whether the final localized state is many-body localized or if the eigenstate thermalization hypothesis (ETH) holds. In the latter case, if the expectation value of local operators will ultimately evolve in time to their value predicted by the microcanonical ensemble [17, 29]. Such a target state, for our system, coincides with a state described by the diagonal ensemble where the spin densities $\rho_{\uparrow,MC}(x)$ and $\rho_{\downarrow,MC}(x)$ are equally distributed. Of course, this cannot happen at infinite interactions: in this limit the system is integrable and the different spins, that are initially spatially phase separated, never mix, making impossible to achieve a uniform non-magnetized state. But at large finite interactions, even if slowly, the spin mixing takes place and continues even after the total density has localized. The long-time position of the center-of-mass of each spin component coincides with the position of the center-of-mass of the whole localized cloud. This is in accordance with what one would expect with the aforesaid fully mixed state where $\rho_{\uparrow,MC}(x) = \rho_{\downarrow,MC}(x)$. Furthermore, since we have verified that the particle densities $\rho^i(x,t)$ and amplitudes $|[a_P(t)]_i|^2$ entering the spin densities (cf. Eq. (10)) possess different relaxation times, in order to investigate the thermalization of the spin dynamics we have evaluated the distance

$$R(t) = \sum_i \left(\sum_{P \in S_N} |[a_P(t)]_i|^2 - \sum_{P \in S_N} |[a_P]_i^{MC}|^2 \right) \quad (22)$$

where $[a_P]_i^{MC}$ are the coefficients obtained from the diagonal ensemble, analogously to what has been done in [17] (see Fig. 5). $R(t)$ collapsing to zero very rapidly, it is clear that, for what concerns the spin density distributions, our system verifies ETH. Thermalization was also reported for spin chains subject to off-diagonal disorder [30]. Our case displays some differences with the above, as the effective disorder felt by the spins is time-dependent, as it originates from the dynamics of the orbital part. It is also interesting to mention that the disorder felt by the particles is diagonal, but it turns off-diagonal as felt by the spins because it is mediated by the interaction among particles.

In conclusion, we would like to emphasize that the center-of-mass evolution of the spin components, namely whether the boomerang dynamics occurs for the spin components, is

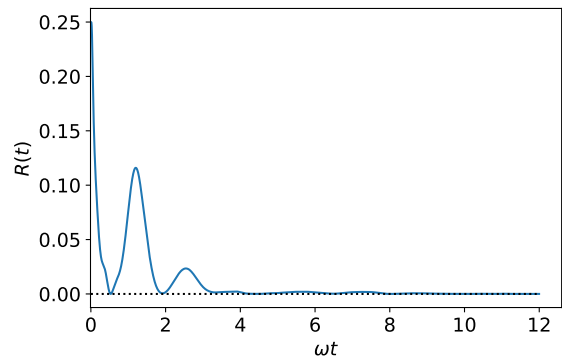


FIG. 5: Distance $R(t)$ from the spin part of the time-dependent average spin density $\bar{\rho}_{\uparrow}(t)$ to the microcanonical one $\rho_{\uparrow,MC}$ as function of time t .

an experimentally accessible tool to probe ETH or lack of thermalization.

V. CONCLUDING REMARKS

In this work we have studied the dynamics of two-component fermionic wavepacket launched in a 1D pseudo-random potential. We have considered the case of an initially spatially phase-separated fermions characterized by a strong repulsive inter-species contact interactions. In such a strongly interacting limit, the charge and the spins dynamics decouple. The total density coincides with the total density of a non-interacting spinless Fermi gas, while the spin components obey to an effective non-homogeneous Heisenberg spin chain Hamiltonian, whose hopping terms, that depend on the density evolution, become random during the dynamics and fluctuate in time. As a result, we find that the total density performs a boomerang dynamics as predicted for non-interacting particles, while the densities of each spin components, considered separately, do not. Their centers of mass initially move away and then they come back, not to their respective initial position, but towards the initial position of the whole system. They reach this position, making damped oscillations, whose frequency is determined by averages of the effective hopping energy. The two spin-components mixed together reach a final spin-density distribution that is compatible with that of the diagonal (microcanonical) ensemble. This is a signature that interactions, in our system, do not induce many-body localization, at least for the parameters that we have chosen for our study. This result is reminiscent of previous studies [29] that have shown that for an Heisenberg spin chain with off-diagonal quenched disorder, many-body localization does not occur. Finally, let us underline that the system we have studied in this work opens up the possibility to realize, with an ultra-cold atom experiment, a quantum simulator of a Heisenberg spin chain with off-diagonal disorder. However, our system differs from that analyzed in [31–34] as the spatial part is subject to a diagonal disorder and the spin components feel an off-diagonal time-dependent disorder. This could bring un-

expected novel phases and deserve further studies for larger systems, correlated disorder and finite temperature.

Acknowledgments

The authors acknowledge the CNRS International Research Project COQSYS for their support, funding from the ANR-21-CE47-0009 Quantum-SOPHA project, support of the Institut Henri Poincaré (UAR 839 CNRS-Sorbonne Université), and LabEx CARMIN (ANR-10-LABX-59-01), and support from the Scientific Research Fund of Piri Reis University under Project Number BAP-2024-04. P. C. acknowledges support from CONICET and Universidad de Buenos Aires, through grants PIP 11220210100821CO and UBACyT 20020220100069BA, respectively. L.T. acknowledges the financial support of the CIC-UMSNH grant n. 18090. The authors acknowledge useful discussions with Dominique Delande, Thierry Giamarchi and Nicolas Laflorencie. They wish to dedicate this paper to Dominique Delande who passed away during the progress of this work.

Appendix A: Two spin dynamics

Let us consider the case of two fermions. In this case, the spin part of the many-body wavefunction can be written on the snippet basis as $a_1(t)|\uparrow\downarrow\rangle + a_2(t)|\downarrow\uparrow\rangle$, with $a_1(t=0) = 1$ and $a_2(t=0) = 0$. There exists only a hopping term J and the a_i 's obey the differential coupled equations

$$i\hbar\dot{a}_{1,2} = -Ja_{1,2} + Ja_{2,1}. \quad (\text{A1})$$

Taking into account that $a_1^2 + a_2^2 = 1$, then we get

$$\begin{aligned} a_1^2 &= \frac{1}{2} \left(1 + \cos\left(2 \int_0^t J(t') dt'\right) \right) \\ a_2^2 &= \frac{1}{2} \left(1 - \cos\left(2 \int_0^t J(t') dt'\right) \right) \end{aligned} \quad (\text{A2})$$

The center-of-mass of each component can be written

$$\begin{aligned} \bar{x}_\uparrow &= \overline{a_1^2 x_1 + a_2^2 x_2} \\ \bar{x}_\downarrow &= \overline{a_2^2 x_1 + a_1^2 x_2} \end{aligned} \quad (\text{A3})$$

where x_1 and x_2 are the baricenters of the density distributions ρ_1 and ρ_2 . We observe that

$$\begin{aligned} \bar{x}_\uparrow &\simeq \overline{a_1^2} \bar{x}_1 + \overline{a_2^2} \bar{x}_2 \\ \bar{x}_\downarrow &\simeq \overline{a_2^2} \bar{x}_1 + \overline{a_1^2} \bar{x}_2. \end{aligned} \quad (\text{A4})$$

Since in the two particles case $\bar{x}_1 = \bar{x}_\uparrow^\infty$ and $\bar{x}_2 = \bar{x}_\downarrow^\infty$, we obtain

$$\bar{x}_{\uparrow,\downarrow} = \frac{1}{2}(\bar{x}_\uparrow^\infty + \bar{x}_\downarrow^\infty) \pm \frac{1}{2}(\bar{x}_\uparrow^\infty - \bar{x}_\downarrow^\infty) \overline{\cos\left(2 \int_0^t J(t') dt'\right)}. \quad (\text{A5})$$

The J 's distribution not being gaussian, the disorder average of the cosine function cannot be written in simple terms, and

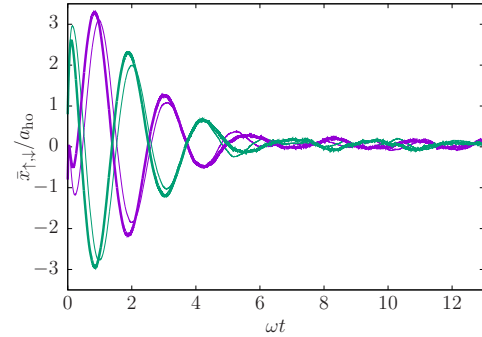


FIG. 6: Spin-up (violet curves) and spin-down (green curves) center-of-mass positions \bar{x}_\uparrow and \bar{x}_\downarrow in units of a_{ho} as functions of the time t , for the case of a two particles systems. The exact results (thick lines) are compared with those obtained using Eq. (A5).

we needed to compute it numerically. Indeed even if \bar{J} determines the spin oscillation frequency, we have verified that the variance σ_j does not allow to deduce a correct damping time. The comparison between the center-of-mass exact evolution and the approximated one given in Eq. (A5) is shown in Fig. 6.

-
- [1] T. Prat, D. Delande, and N. Cherroret, *Physical Review A* **99**, 023629 (2019), ISSN 2469-9926, 2469-9934, URL <https://link.aps.org/doi/10.1103/PhysRevA.99.023629>.
- [2] L. Tessieri, Z. Akdeniz, N. Cherroret, D. Delande, and P. Vignolo, *Physical Review A* **103**, 063316 (2021), ISSN 2469-9926, 2469-9934, URL <https://link.aps.org/doi/10.1103/PhysRevA.103.063316>.
- [3] R. Sajjad, J. L. Tanlimco, H. Mas, A. Cao, E. Nolasco-Martinez, E. Q. Simmons, F. L. N. Santos, P. Vignolo, T. Macrì, and D. M. Weld, *Phys. Rev. X* **12**, 011035 (2022), URL <https://link.aps.org/doi/10.1103/PhysRevX.12.011035>.
- [4] P. W. Anderson, *Phys. Rev.* **109**, 1492 (1958), URL <https://link.aps.org/doi/10.1103/PhysRev.109.1492>.
- [5] E. Abrahams, P. W. Anderson, D. C. Licciardello, and T. V. Ramakrishnan, *Phys. Rev. Lett.* **42**, 673 (1979), URL <https://link.aps.org/doi/10.1103/PhysRevLett.42.673>.
- [6] F. Noronha and T. Macrì, *Phys. Rev. B* **106**, L060301 (2022), URL <https://link.aps.org/doi/10.1103/PhysRevB.106.L060301>.
- [7] F. Noronha, J. A. S. Lourenço, and T. Macrì, *Phys. Rev. B* **106**, 104310 (2022), URL <https://link.aps.org/doi/10.1103/PhysRevB.106.104310>.

- 10.1103/PhysRevB.106.104310.
- [8] J. Janarek, B. Grémaud, J. Zakrzewski, and D. Delande, *Phys. Rev. B* **105**, L180202 (2022), URL <https://link.aps.org/doi/10.1103/PhysRevB.105.L180202>.
- [9] J. Janarek, D. Delande, N. Cherroret, and J. Zakrzewski, *Physical Review A* **102**, 013303 (2020), ISSN 2469-9926, 2469-9934, URL <https://link.aps.org/doi/10.1103/PhysRevA.102.013303>.
- [10] J. Janarek, J. Zakrzewski, and D. Delande, *Phys. Rev. B* **107**, 094204 (2023), URL <https://link.aps.org/doi/10.1103/PhysRevB.107.094204>.
- [11] I. Basko, D.M.; Aleiner and B. Altshuler, *Ann. of Phys.* p. 1126 (2006), URL <https://doi.org/10.1016/j.aop.2005.11.014>.
- [12] J. Zakrzewski and D. Delande, *Phys. Rev. B* **98**, 014203 (2018), URL <https://link.aps.org/doi/10.1103/PhysRevB.98.014203>.
- [13] T. Kohlert, S. Scherg, X. Li, H. P. Lüschen, S. Das Sarma, I. Bloch, and M. Aidelsburger, *Phys. Rev. Lett.* **122**, 170403 (2019), URL <https://link.aps.org/doi/10.1103/PhysRevLett.122.170403>.
- [14] F. Deuretzbacher, D. Becker, J. Bjerlin, S. M. Reimann, and L. Santos, *Phys. Rev. A* **90**, 013611 (2014), publisher: American Physical Society, URL <https://link.aps.org/doi/10.1103/PhysRevA.90.013611>.
- [15] L. Yang, L. Guan, and H. Pu, *Phys. Rev. A* **91**, 043634 (2015), URL <https://link.aps.org/doi/10.1103/PhysRevA.91.043634>.
- [16] L. Yang and H. Pu, *Phys. Rev. A* **94**, 033614 (2016), URL <https://link.aps.org/doi/10.1103/PhysRevA.94.033614>.
- [17] G. Pecci, P. Vignolo, and A. Minguzzi, *Phys. Rev. A* **105**, L051303 (2022), URL <https://link.aps.org/doi/10.1103/PhysRevA.105.L051303>.
- [18] M. Ljubotina, M. Žnidarič, and T. c. v. Prosen, *Phys. Rev. Lett.* **122**, 210602 (2019), URL <https://link.aps.org/doi/10.1103/PhysRevLett.122.210602>.
- [19] E. Ilievski, J. De Nardis, M. Medenjak, and T. c. v. Prosen, *Phys. Rev. Lett.* **121**, 230602 (2018), URL <https://link.aps.org/doi/10.1103/PhysRevLett.121.230602>.
- [20] J. De Nardis, M. Medenjak, C. Karrasch, and E. Ilievski, *Phys. Rev. Lett.* **123**, 186601 (2019), URL <https://link.aps.org/doi/10.1103/PhysRevLett.123.186601>.
- [21] D. Wei, A. Rubio-Abadal, B. Ye, F. Machado, J. Kemp, K. Srakaew, S. Hollerith, J. Rui, S. Gopalakrishnan, N. Y. Yao, et al., *Science* **376**, 716 (2022), URL <https://www.science.org/doi/10.1126/science.abk2397>.
- [22] A. G. Volosniev, D. V. Fedorov, A. S. Jensen, M. Valiente, and N. T. Zinner, *Nature Communications* **5**, 5300 (2014), ISSN 2041-1723, URL <https://doi.org/10.1038/ncomms6300>.
- [23] J. Decamp, P. Armagnat, B. Fang, M. Albert, A. Minguzzi, and P. Vignolo, *New J. Phys.* p. 055011 (2016).
- [24] R. E. Barfknecht, A. Foester, and N. T. Zinner, *Scientific Reports* **9**, 15994 (2019), URL <https://doi.org/10.1038/s41598-019-52392-2>.
- [25] M. Griniasty and S. Fishman, *Phys. Rev. Lett.* **60**, 1334 (1988), URL <https://link.aps.org/doi/10.1103/PhysRevLett.60.1334>.
- [26] M. Schreiber, S. SEAN S. Hodgman, P. Bordia, H. Lüschen, M. Fischer, R. Vosk, E. Altman, U. Schneider, and I. Bloch, *Science* **349**, 842 (2015), URL <https://www.science.org/doi/10.1126/science.aaa7432>.
- [27] K. A. Matveev, *Phys. Rev. B* **70**, 245319 (2004), URL <https://link.aps.org/doi/10.1103/PhysRevB.70.245319>.
- [28] F. Deuretzbacher, D. Becker, and L. Santos, *Phys. Rev. A* **94**, 023606 (2016), publisher: American Physical Society, URL <https://link.aps.org/doi/10.1103/PhysRevA.94.023606>.
- [29] F. Alet and N. Laflorencie, *Comptes Rendus Physique* **19**, 498 (2018), URL <https://doi.org/10.1016/j.crhy.2018.03.003>.
- [30] D. J. Luitz, N. Laflorencie, and F. Alet, *Phys. Rev. B* **91**, 081103 (2015), URL <https://link.aps.org/doi/10.1103/PhysRevB.91.081103>.
- [31] N. Laflorencie and H. Rieger, *Phys. Rev. Lett.* **91**, 229701 (2003), URL <https://link.aps.org/doi/10.1103/PhysRevLett.91.229701>.
- [32] N. Laflorencie and H. Rieger, *Eur. Phys. Journ. B* p. 201 (2004).
- [33] N. Laflorencie, H. Rieger, A. W. Sandvik, and P. Henelius, *Phys. Rev. B* **70**, 054430 (2004), URL <https://link.aps.org/doi/10.1103/PhysRevB.70.054430>.
- [34] N. Laflorencie, *Phys. Rev. B* **72**, 140408 (2005), URL <https://link.aps.org/doi/10.1103/PhysRevB.72.140408>.